ALMA MEMO No. 361

PHASE CROSS-CORRELATION OF A 11.2 GHZ INTERFEROMETER AND 183 GHZ WATER LINE RADIOMETERS AT CHAJNANTOR

Guillermo Delgado
Onsala Space Observatory / European Southern Observatory
Casilla 19001, Santiago 19, Chile
Email: gdelgado@eso.org

Lars-Åke Nyman
Onsala Space Observatory / European Southern Observatory
Casilla 19001, Santiago 19, Chile
Email: lnyman@eso.org

Angel Otárola
European Southern Observatory
Casilla 19001, Santiago 19, Chile
Email: aotarola@eso.org

Richard Hills
Mullard Radio Astronomy Observatory
Cavendish Laboratory, Cambridge CB3 OHE, UK
Email: richard@mrao.cam.ac.uk

Yasmin Robson
Mullard Radio Astronomy Observatory
Cavendish Laboratory, Cambridge CB3 OHE, UK
Email: yr@astro.ox.ac.uk

Abstract – The phase variation from a 300-m baseline 11.2 GHz interferometer was cross-correlated with the phase variation estimated from the PWV measurements using two radiometers operating near the water vapour line at 183 GHz at the ALMA site of Llano de Chajnantor in Northern Chile at an altitude of 5,000 m. Care has been taken to have the radiometers observing the same path of atmosphere as the interferometers, with both beams matched as close as possible.

The result indicates that the cross-correlation varies during the day and thus the phase correction possible to achieve using the radiometric method at Chajnantor.

The results are discussed and comparisons are done with other variables, specially the height of the turbulence layer. The later is determined using two different methods: the first one is direct measurements from radiosonde data, and the second method involves the calculation of the time lag between the turbulence structures seen by the two interferometers deployed at Chajnantor. A relation is proposed between the height of the turbulence layer and the success of the cross-correlation, with a better cross-correlation when the turbulence layer is higher than about 300-400 m.

1 Introduction

Phase decorrelation due to water vapour in the atmosphere decreases both the sensitivity and resolution of an interferometer operating at millimetre and sub-millimetre wavelengths. It is therefore necessary to perform a phase correction of the astronomical signal.

The principle behind the phase correction experiment at the ALMA site of Chajnantor is described in Figure 1 and shows a plane wave originating on a point over the atmosphere. Its phase front is delayed selectively by the change of the refractivity at the lower atmosphere (troposphere) due to the presence of water vapour. Because water vapour does not mix well with the other atmospheric gaseous components, the variation of the refractivity will follow the water vapour variations crossing in front of the interferometer beam. These water vapour cells will also present a thermal emission that can be detected by a radiometer. If we assume that the thermal emission is proportional to the amount of PWV contained in the line-of-sight column, then the PWV variations will reflect the displacement of the water vapour cells in front of the radiometer beam.

Small-scale PWV variations give rise to pathlength variations that translate linearly to phase fluctuations. The radiometric measurement of these *PWV* variations can be used to predict the tropospheric phase fluctuation due to water vapour. This value subtracted from the interferometer phase fluctuation can effectively reduce the phase decorrelation. This method has been applied before to interferometric measurements done at Mauna Kea by Wiedner [1], Yun & Wiedner [2] and Delgado *et al.* [3] and also at Chajnantor by Delgado *et al.* [4].

Here we will discuss some results obtained for Chajnantor, concentrating our work on the first three weeks of November 1999. During this period, a radiosonde campaign was made with several launches per day between 5-11 November 1999. Because of power problems in the ESO instrumentation container, the data does not overlap for all instruments over the complete period.

2 Phase cross-correlation between 11.2 GHz interferometer and 183 GHz water line radiometer

The experimental setup at Chajnantor has been described by Delgado *et al.* [3, 4]. It is sufficient to say here that the 183 GHz water line radiometers share a 300-m baseline with a 11.2 GHz interferometer observing the CW beacon of a commercial satellite at an elevation of ~35° in the NE direction.

It is important to remind the reader that the measurements shown here are obtained with the same setup described in [4], this is a flat mirror on the 183 GHz water line radiometers producing a beam of ~2.5°, compared with a beam of ~1° for the 11.2 GHz interferometer. The distance between the 183 GHz water line

radiometers and the 11.2 GHz interferometer antennas is ~6 m, with a measured offset between radiometer and interferometer beams of 27' (Figure 2).

The amount of PWV is estimated from antenna temperature measurements at three different frequencies close to the centre of the 183.31 GHz water line emission frequency, as explained elsewhere [3, 4].

From the PWV value, a pathlength variation is estimated using a linear relation between the two quantities (1 mm of PWV increases by 6.3 mm the pathlength) [5]. Because the atmosphere away from line centres is highly non-dispersive at millimetre frequencies, we can use this pathlength value to calculate the phase variation at any frequency.

The raw phase variation data measured by the 11.2 GHz interferometer, is sampled at a 1-second rate and divided in 10-minute blocks. A second order baseline is removed from the data sets to remove the effect of the orbital drift of the satellite from the antenna beam centres and any existing instrumental drift.

The 183 GHz water line radiometer produces one measurement every 2 seconds. Since the time series of both instruments are different, we have to interpolate the data. For this, we use the time stamp of the 183 GHz water line radiometer as reference. This means that the resulting time series used to calculate the cross-correlation has a 2 seconds sample interval.

The resulting time series for each day is divided in 10-minute blocks and, after a linear baseline removal to the radiometer data, both signals are cross-correlated, calculating at the same time the variance of each of them. This cross-correlation is based on a least squares fitting to a linear relation between the interferometer phase ($\Delta\phi_{interferometer}$ independent variable) and the radiometer phase ($\Delta\phi_{radiometer}$ dependent variable). This is:

$$\Delta\phi_{radiometer} = a + b\,\Delta\phi_{interferometer} \qquad (1)$$

Ideally the offset coefficient *a* should be zero, the linear coefficient *b* should be one, and the correlation coefficient *r* between both time series should also be unity. The correlation coefficient, or Pearson's *r*, is given by [6]:

$$r = \frac{\sum_i \left[\left(\Delta\phi_{interferometer_i} - \left\langle \Delta\phi_{interferometer} \right\rangle\right)\left(\Delta\phi_{radiometer_i} - \left\langle \Delta\phi_{radiometer} \right\rangle\right)\right]}{\sqrt{\sum_i \left(\Delta\phi_{interferometer_i} - \left\langle \Delta\phi_{interferometer} \right\rangle\right)^2}\ \sqrt{\sum_i \left(\Delta\phi_{radiometer_i} - \left\langle \Delta\phi_{radiometer} \right\rangle\right)^2}} \qquad (2)$$

We calculated the cross-correlation of all the available data for the period 1-21 of November 1999. The coverage is not complete because we experienced problems with the electro-voltaic system powering the ESO instrumentation at Chajnantor. The result for the daily calculated cross-correlation shows large variations in shapes (Figure 3).

3 Analysis of the average cross-correlation

From Figure 3 it is not possible to reach too many conclusion about the result of the cross-correlation between interferometer and radiometer phase and other variables due to the wide range of daily responses. Still, there is a trend indicating that the cross-correlation is better in the second half of the day. Figure 4, shows the average value for the cross-correlation coefficient for all the available data for the period 1-21 of November 1999, the scale shows the UT time. Local time is 4 hours behind UT time.

It can be seen that at around 8 AM local time (immediately after sunrise) the cross-correlation improves to reach a flat maximum of about 8 hours. At around 8 PM local time (immediately after sunset), the cross-correlation starts deteriorating very rapidly, to reach a flat minimum of about 12 hours. The rest of the time, the cross-correlation is changing between one of the two very distinct states.

To understand the origin of the cross-correlation trend shown on Figure 4, we can look at a study case using day 15/11/99, this day is representative of the "average" behaviour, and is useful to illustrate the main characteristics of both time series for the phase variation and the cross-correlation result.

In Figure 5 we have the phase variation seen by the interferometer and the radiometer during this day and also the cross-correlation is repeated here for convenience. At the beginning of the UT day, between roughly 8 PM local time (previous day) and 3:00 AM local time the interferometer "sees" a high frequency phase fluctuation with larger amplitude as compared with the 183 GHz water line radiometer. During this time the cross-correlation is small. Later that day, for about 5-6 hours (between roughly 3:00 AM local time and 8:30 AM local time) the phase variations for both instruments are very small. During this time the cross-correlation between the phase signals improves but remains at a relatively low value.

The second half of the UT day (starting at 8:30 AM, local time) presents a more unstable condition, with a larger amplitude of the phase variations. Both instruments agree quite closely in the general characteristic of this phase variation. This is reflected in the higher cross-correlation during this time of the day. The amplitude does not show a good agreement.

More detailed examples of the phase variation of both instruments can be seen in Figure 6, where we have 10 minutes snap-shots of three representative moments of the day at a) 4:22:27 UT (0:22:27 local time), b) 7:58:37 UT (3:58:37 local time), and c) 15:43:32 UT (11:43:32 local time).

At the time of low correlation (0:22:27 local time), it can be seen that the interferometer high frequency phase noise dominates, with the radiometer having a low amplitude and frequency response (Figure 6 a)).

When the cross-correlation starts to improve (3:58:37 local time), both signals tend to agree on the trend presenting also some periods with obvious discrepancies and some disagreement on the relative amplitude of the phase given by the two instruments (Figure 6 b)). The absolute amplitude of the phase variation remains low at this time, comparable with those amplitudes at the time of low correlation.

At the time of higher cross-correlation (11:43:32 local time), the amplitude of the phase variations has increased by an order of magnitude with respect to the previous samples (Figure 6 c)). The trend is followed very closely by both instruments, with the amplitude still differing between them. This is reflected in the better value for the cross-correlation.

Low correlation at the beginning of the day is due to two different phenomena. On one hand we have the high frequency phase noise on the interferometer for some periods, and on the other hand the lack of a good agreement between the phase signals as given by the two instruments during the time when the amplitude of the phase variations are small.

Lower plot of Figure 5 shows the linear coefficient *b* in equation (1) of the sample day (15/11/99). This is highly correlated with the cross-correlation plot. It can be confirmed that the linear coefficient in the best case reaches around 0.7, indicating that the radiometer phase is underestimated by about 40% as compared with the interferometer phase. Furthermore, this linear coefficient varies during the day. This effect will not be discussed here.

4 Correlation of the results with other variables

The average cross-correlation coefficient shown in Figure 4, is compared with some atmospheric variables. While there might be many other possible variables to correlate, here we investigated the most relevant ones.

4.1 Amount and daily cycle of PWV

A natural starting approach to understand the daily cycle of the average cross-correlation coefficient is to compare the cross-correlation with the amount of PWV at the moment of the measurements.

Figure 7 shows the line of sight PWV (heavy line) and the cross-correlation coefficient (light line) for days 06/11/99 and 15/11/99. These two days are interesting because they are very different (similar?) in behaviour, with 06/11/99 showing a high PWV content during the whole day, and a lower relative PWV content at the end of the day, while day 15/11/99 presents a PWV content that is lower than that of day 06/11/99 and, opposite as the case for day 06/11/99, shows a higher PWV content by the end of the day.

Despite the very different behaviour of the PWV during both days, the cross-correlation between the phase variation measured with the interferometer and the radiometer is very similar over the day for both days (low cross-correlation at the beginning of the day, to improve latter on the second half of the day), showing no apparent cross-correlation, either with the PWV amount or the particular distribution of it during the day. The profile of the phase variation is very similar on both days (Figure 8), with a lower phase noise during the first half of the day (local night-time) and higher phase noise during the second half of the day (local day-time).

In conclusion the success of the phase correction for this experimental set-up is not related to the amount of PWV or its diurnal change.

4.2 Weather variables

Average weather variables during the observed period compared with the average distribution of the cross-correlation coefficient show no apparent correlation, except for the case of solar irradiation (Figure 9 a)), and even more clearly with ground temperature. This is shown in Figure 9 b), indicating that as average temperature crosses about –4° C, the cross-correlation starts to improve. Day-to-day departures from this average trend indicate that this might not be a direct relation, but rather through some other atmospheric variable related to the temperature.

4.3 Height of the turbulence layer

The height of the turbulence layer is an interesting variable to explore because it presents a daily cycle, related to the solar radiation (temperature?).

At Chajnantor there are two sets of 11.2 GHz interferometers. One installed by NRAO in 1995 and a second one installed by ESO during 1998. These instruments are identical interferometers, sharing a 300-m baseline, but observing different satellites at similar frequencies. The two observed satellites have different sky positions and thus the interferometer beams are pointing towards different elevations.

One method of determining the height of the turbulence layer is by using the information from two sets of interferometers. The idea is to determine the time lag between the structures seen in the phase time series at both interferometers and, by assuming that the turbulent layer has the same speed and direction as the wind speed and direction measured at ground level, the known geometry of the interferometers allows the determination of the altitude of the turbulence layer [7]. The principles of the interferometer are described in [8], while the geometry of the method is described on [9].

Another method of estimating the height of the turbulence layer is by observing the temperature anomalies in the radiosonde profiles indicating inversion layers. These layers, trapping the water vapour cells, are probably the sites where turbulence is originated.

For some radiosonde flights we have more than one value associated with the radiosonde-determined turbulence height. This may be due to the presence at that time of more than one inversion layer. The dominant turbulence layer is assumed to be the one closer to the ground, since the higher layers should only contain a small fraction of the water vapour. We have done a comparison between the direct measurement of the altitude of the turbulence layer from the radiosonde flights and the estimation using the two-interferometer technique (Figure 10). The result shows that the general trend is indicated by both instruments. There is still a question about the relative altitude of the turbulence layer as indicated by both instruments at different times. There does not seem to be a systematic difference in the magnitude of the height as determined with both methods, thus we can not interpret this difference as a systematic geometrical error. From Figure 10 it seems that the turbulence layer varies with a daily cycle, with lower heights of the turbulence layer at the beginning of the UT day (local night-time), to increase during the local day-time.

A comparison was done between the height of the turbulence layer determined by the two-interferometer method and the cross-correlation coefficient, between the phase variation measured by the interferometer and the one estimated by the radiometer. The result shown in Figure 11, indicates that there seems to be a tendency to have a better cross-correlation during those times when the turbulence layer is over about 300-400 m. The covered period is for the radiosonde launches between November 5 and 9 1999.

5 Discussion and conclusions

We have found that the degree of correlation between the phase variation, measured with the 11.2 GHz interferometer and the 183 GHz radiometer, varies during the day. This variation is different day-to-day, but a general trend is clear. The cross-correlation coefficient seems to be related to temperature or some other atmospheric variable related to temperature. One proposed relation is with the altitude of the turbulence layer: it appears that the degree of correlation improves when the turbulence layer is at heights larger than about 300-400 m. This might be a limitation of our actual experimental setup at Chajnantor since Robson *et al.* [7] have determined that about 70% of the time the turbulence layer is bellow 500 at Chajnantor.

The main problem with a turbulence layer too close to the ground is because of the different far-field distances for the two instruments. For the case of a radiometer, operating at 183 GHz, the far-field distance is very short (millimetres). Whereas for the interferometer, considering an operating frequency of 11.2 GHz and a diameter of 1.8 m, the far field distance is of the order of 250 m and, even when the satellite signal is in the far-field of the interferometer, the perturbing phase screen of water vapour can be within the near-field. This means that the size and shape of the antenna beam pattern will be very different for the two instruments depending on the distance from the ground.

The periods when the turbulent layer is close to the ground seem to correspond to the local night-time. This is also the time of the day when the atmospheric phase noise is minimum. These two effects are present at the same time and might be the reason why the cross-correlation between the interferometer and the radiometer phase is low during this time of the day.

During this work we also detected other problems that need a better understanding for the success of the phase correction method as applied here. Some of the problem that need to be addressed are:

- The dynamics of the turbulence layer needs to be determined in a better way for Chajnantor. We already know that this height varies with a daily cycle, but we need to relate this height change to other variables. Especially desirable will be the relation of this height with meteorological variables. We need to develop a more reliable and constant method to measure the height of this turbulence layer.
- There is a relative amplitude difference between interferometer phase data and radiometer phase data, with the radiometer phase systematically lower than the interferometer measured phase data. Here we need to investigate the water line model being used and the linear relation between pathlength and phase variation.
- In the interferometer data during some days we found the presence of a high frequency phase variation lasting for a few hours. This phase noise shows a high frequency characteristic and is not present at all times. Preliminary investigation of this indicates an ionospheric origin. Here we need to proceed with a careful analysis of historical data to assert the relative relevance of these periods. If this noise is convincingly demonstrated to have an ionospheric origin, this poses a serious limitation to the experimental setup at Chajnantor because of the impossibility to directly separate the ionospheric phase noise from the tropospheric (PWV) phase noise. On the other hand, if this noise is indeed of ionospheric origin, it does not present a problem for ALMA since the phase correction and observations will be conducted at much higher frequencies.
- We need to guarantee the continuous output of data of all the instruments involved in the phase correction experiments (radiometers, interferometers (both ones), weather stations, etc.) and also we need more radiosonde campaigns, with night flights. This is particularly relevant to attempt a correlation between the

success of the phase correction method and local weather conditions, considering probable limitations of the experimental setup at Chajnantor.

- The problem of the different beam sizes has been recently solved by replacing the flat mirror of the radiometer by curved mirrors producing a beam about the same size as the interferometers. Now a high priority task is to properly align the beam of the two instruments.

Acknowledgements

This work is the result of a collaborative work between many different people and institutions at both sides of the Atlantic. Professor Roy Booth (OSO) was instrumental on the building and deployment of these instruments at Chajnantor. Victor Belitzky and Denis Urbain (OSO) build the radiometers in collaboration with the staff from MRAO. Martina Wiedner (SAO) wrote most of the original water line modelling code and we profited extensively of her excellent work. The staff of NRAO has been very important in the construction and functioning of the two 11.2 GHz interferometers (radio seeing monitors) deployed at Chajnantor.

Important part of the funding for this project came out of the budget of Onsala Space Observatory provided by the Swedish Natural Science Council (NFR).

References

[1] M. Wiedner, PhD thesis, 1998.

[2] M. Yun and M. Wiedner, “Phase Correction using 183 GHz Radiometers during the Fall 1998 CSO-JCMT Interferometer Run,” ALMA Memo Series No. 252, 1999.

[3] G. Delgado, A. Otárola, V. Belitsky, D. Urbain, and P. Martin-Cocher, “The Determination of Precipitable Water Vapour at Llano de Chajnantor from Observations of the 183 GHz Water Vapour Line,” ALMA Memo Series No. 271, 1999.

[4] G. Delgado, A. Otárola, L-Å. Nyman, , R. Booth, V. Belitsky, D. Urbain, R. Hills, Y. Robson, and P. Martin-Cocher, “Phase Correction of Interferometer Data at Mauna Kea and Chajnantor,” ALMA Memo Series No. 332, 2000.

[5] A. Thompson, J. Moran, and G. Swenson, *Interferometry and Systhesis in Radio Astronomy*, Krieger Publishing Company, 1994.

[6] W. Press, B. Flannery, S. Teukolsky, and W. Vetterling, *Numerical Recipes in C: the Art of cientific Computing*, Cambridge University Press, 1992.

[7] Y. Robson, R. Hills, J. Richer, G. Delgado, L-Å. Nyman, A. Otárola, and S. Radford, “Phase Fluctuations at the ALMA Site and the Height of the Turbulent Layer,” to be published in the Proeedings of the IAU-2000 Conference, 2000.

[8] S. Radford, G. Reiland, and B. Shillue, “Site Test Interferometer,” PASP, Vol. No. 108, pp. 441-445, 1996.

[9] M. Holdaway and S. Radford, “Options for Placement of a Second Site Test Interferometer on Chajnantor,” ALMA Memo Series No. 196, 1998.

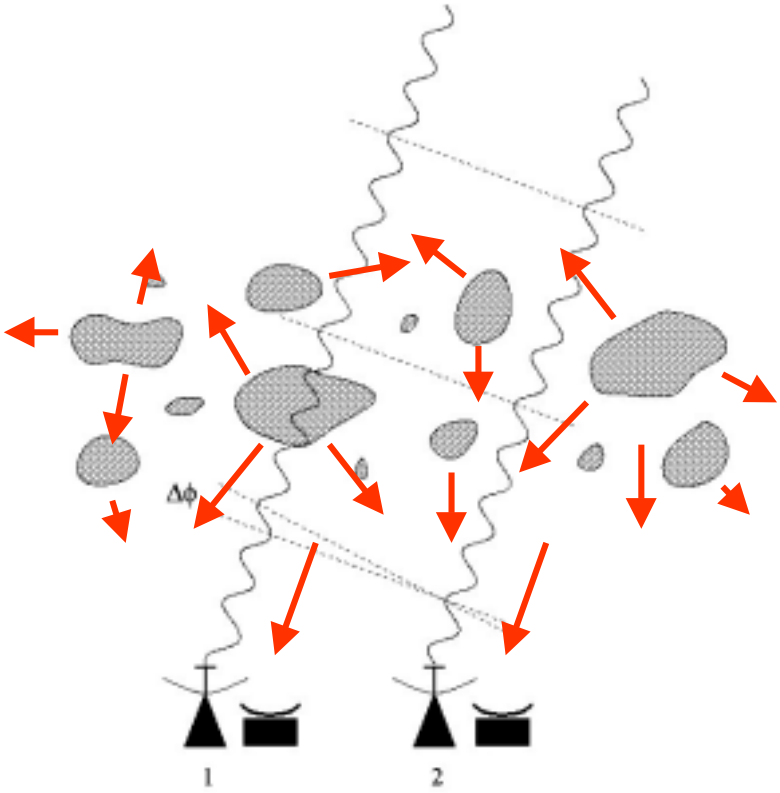

Fig 1.- Experimental setup at Chajnantor where two identical radiometers are situated at the ends of a 300-m baseline of an interferometer operating at 11.2 GHz. The interferometer measures the phase variations of a plane wave coming from a geostationary satellite and the radiometer measures the thermal emission at the water line emission frequency.

Fig 2.- The experimental setup at Chajnantor showing one end of the interferomeer baseline. The 183 GHz radiometer is on the right, the ESO dish is at the centre and the NRAO dish on the left. The distance between the radiometer and the NRAO interferometer used for the experiment described here is of about 6 m.

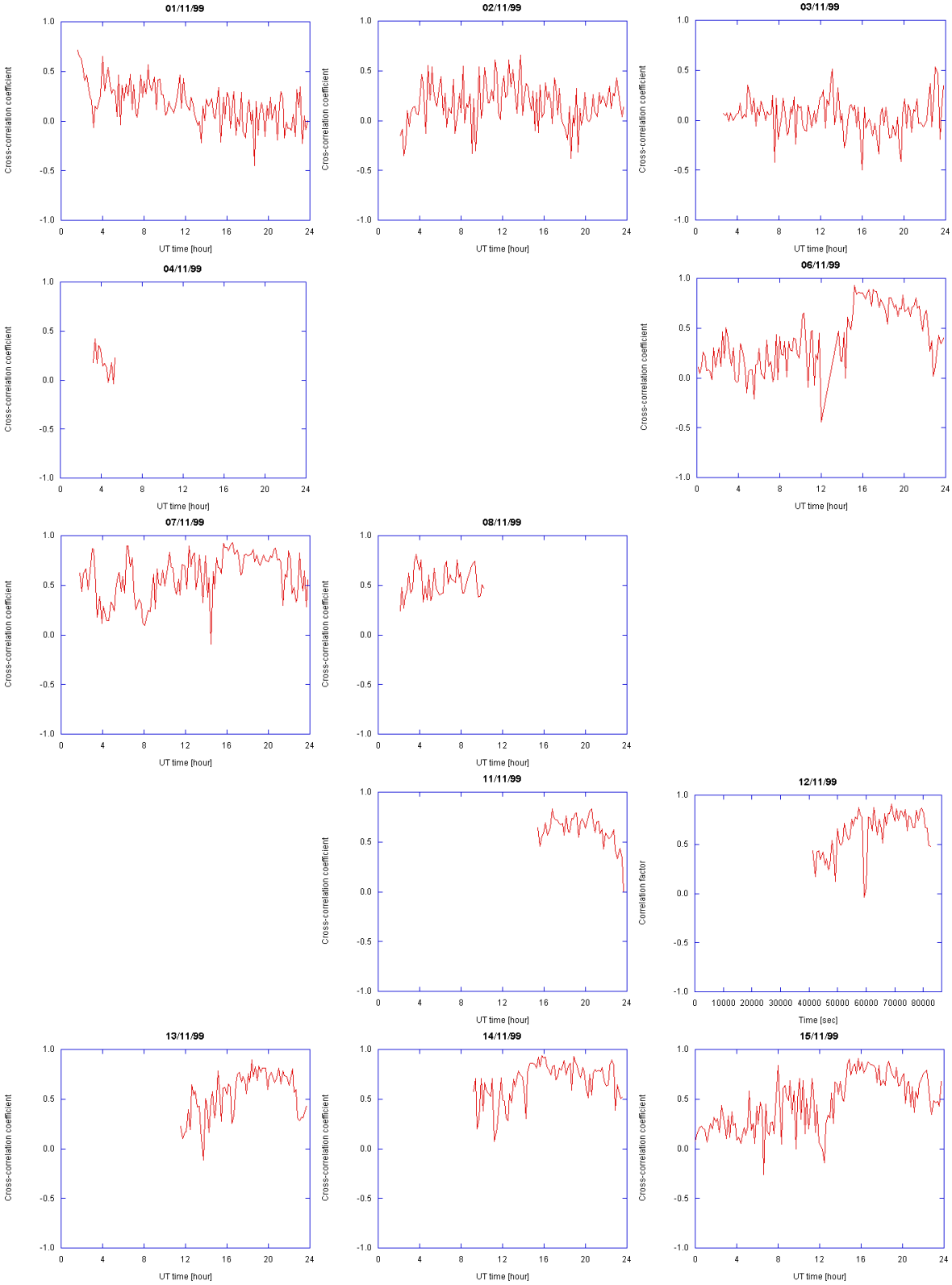

Figure 3.- Cross-correlation of a linear relation between interferometer measured phase and radiometer estimated phase.

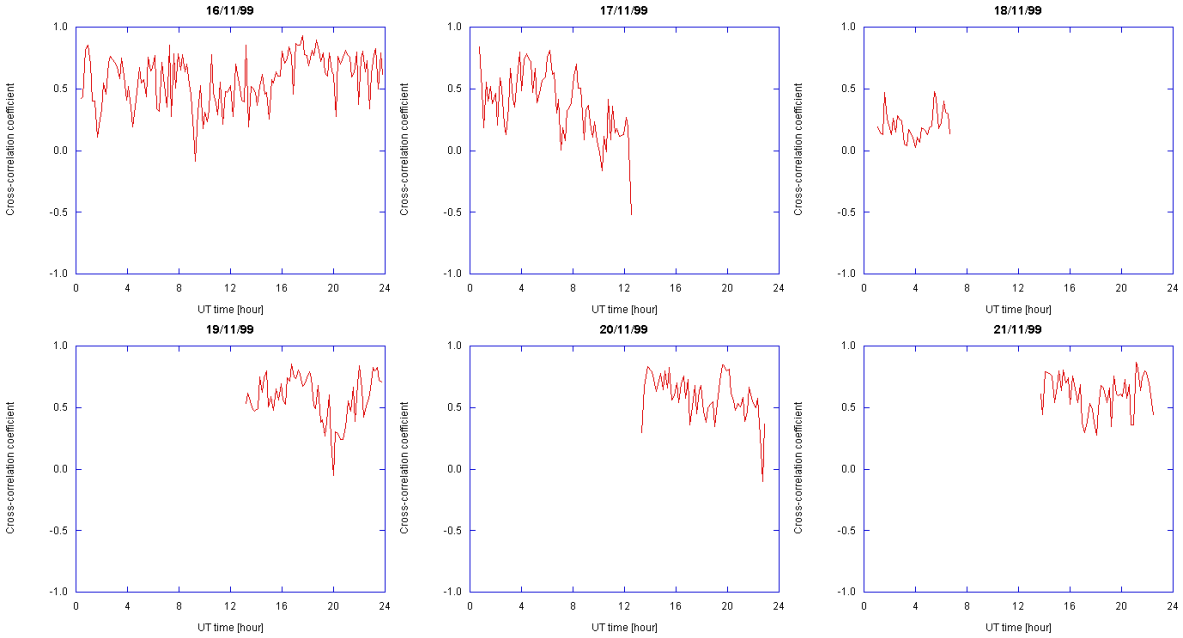

Figure 3.- (Cont.) Cross-correlation of a linear relation between interferometer measured phase and radiometer estimated phase.

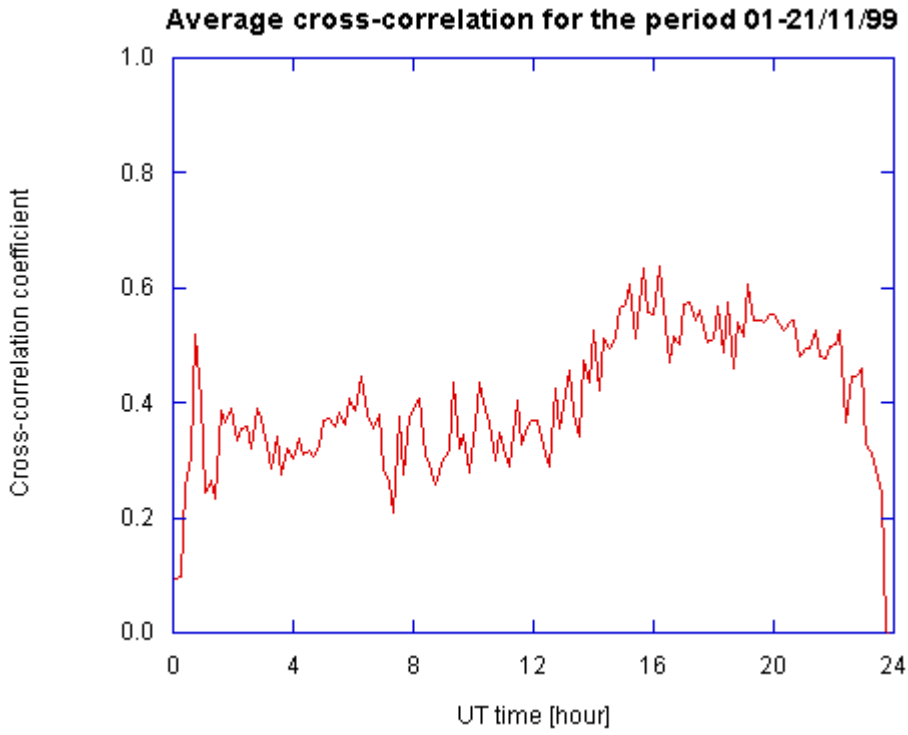

Figure 4.- Average correlation coefficient for the available data on the period 1-21/11/99.

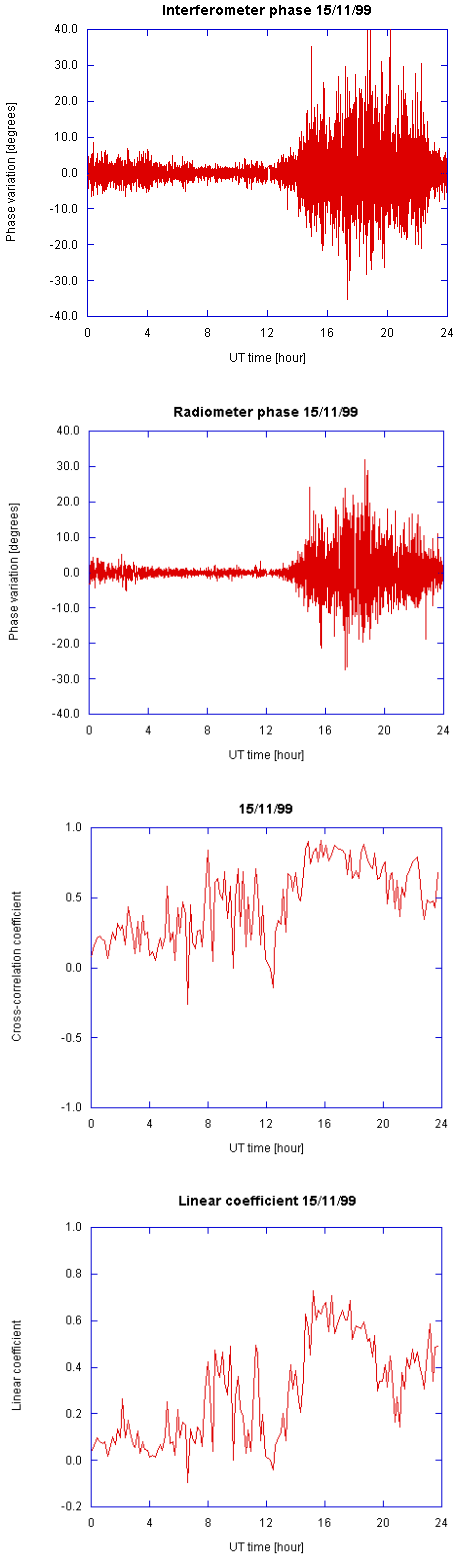

Figure 5.- Phase variation for the 15/11/99 measured on a 300-m baseline for the 11.2 GHz interferometer (upper plot) and the 183 GHz water line radiometer (second plot from above). The cross-correlation coefficient for the same period is also shown (third plot from above) as well as the linear coefficient corresponding to the linear least squares fitting (lower plot). At around 12 UT there is a period of about one hour with no data.

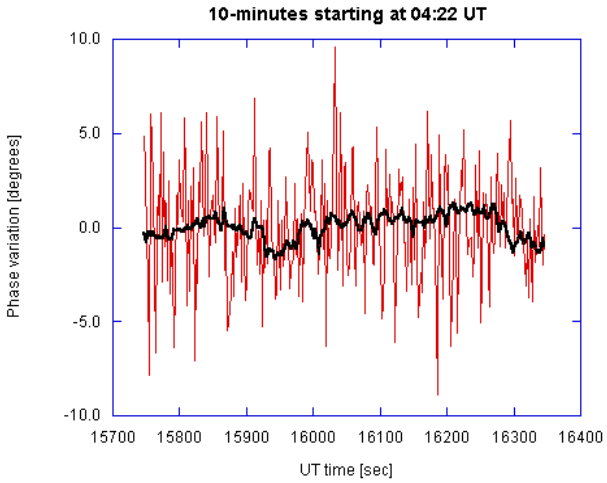

a)

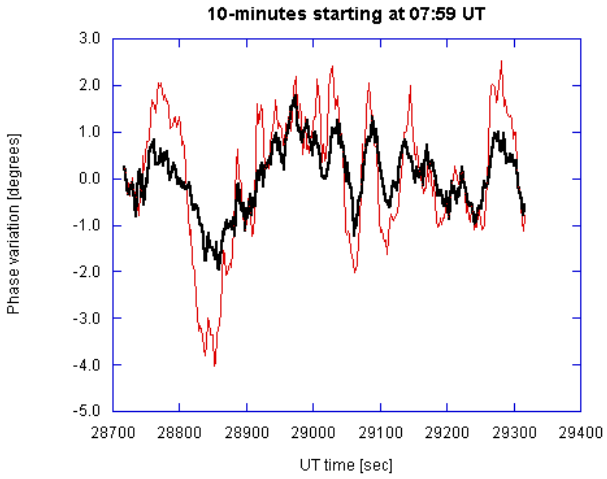

b)

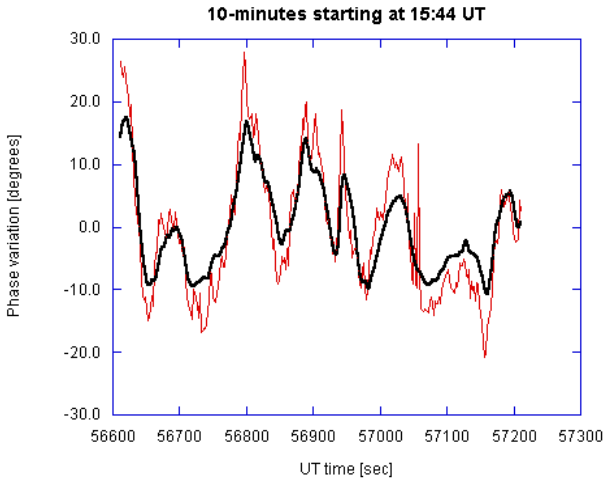

c)

Figure 6.- 10 minute snap-shots of representative times for the phase variation. The thick line is the radiometer estimated phase and the thin line is the interferometer measured phase.

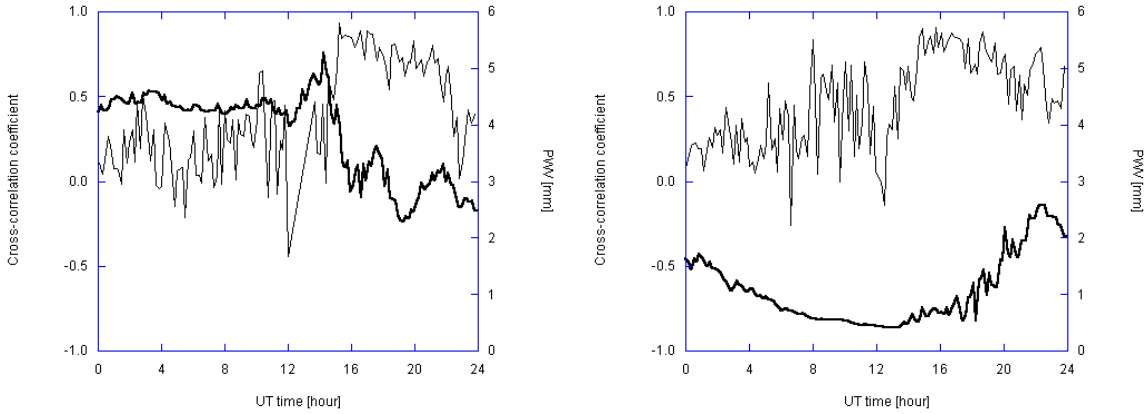

Figure 7.- PWV [mm] along the line of sight (heavy line) and the cross-correlation coefficient (light line) for day 06/11/99 (left plot) and 15/11/99 (right plot).

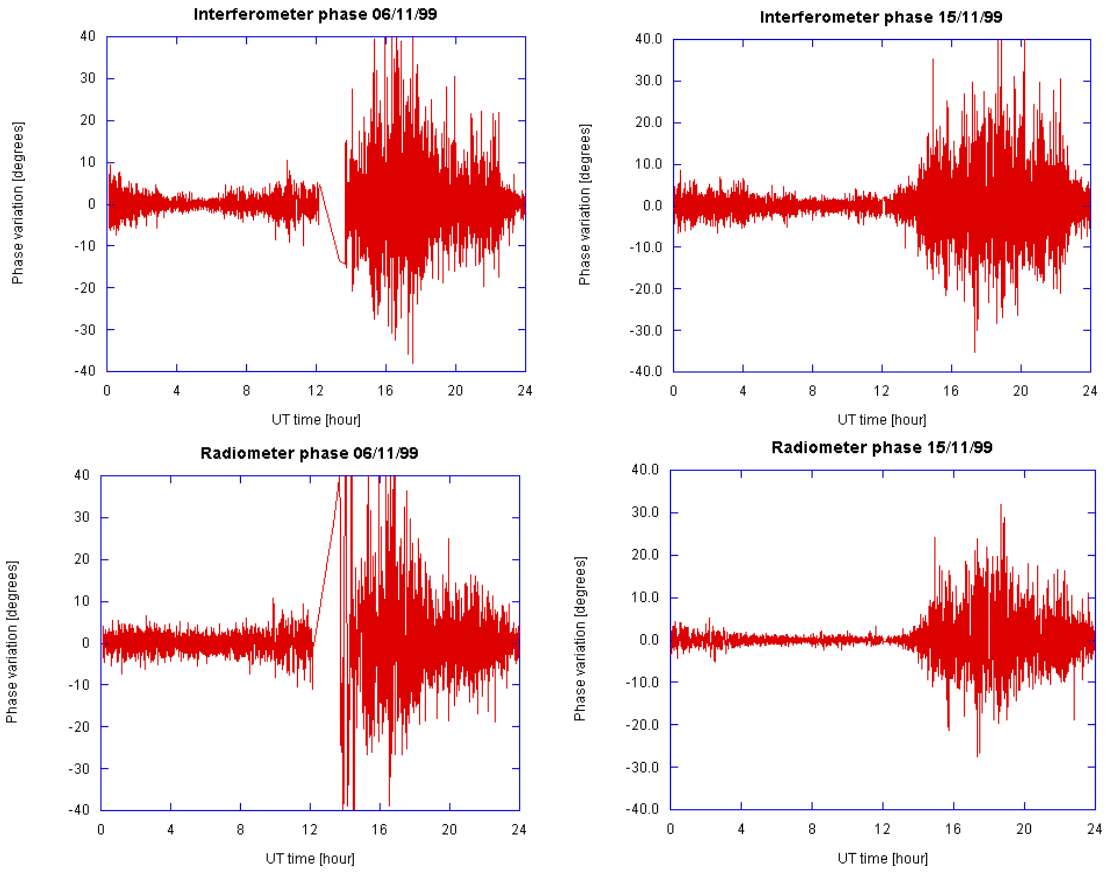

a) b)

Fig 8.- Phase variation for day a) 06/11/99 and b) 15/11/99. The upper plots represent the phase variation measured by the 11.2 GHz interferometer and the lower plots the phase variation estimated by the radiometers

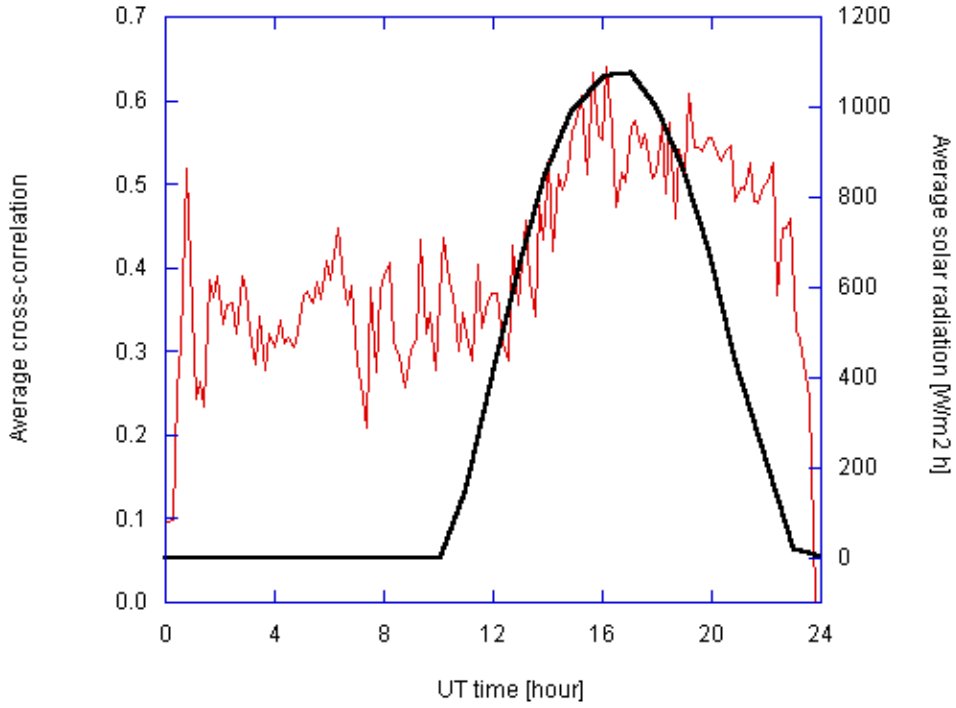

a)

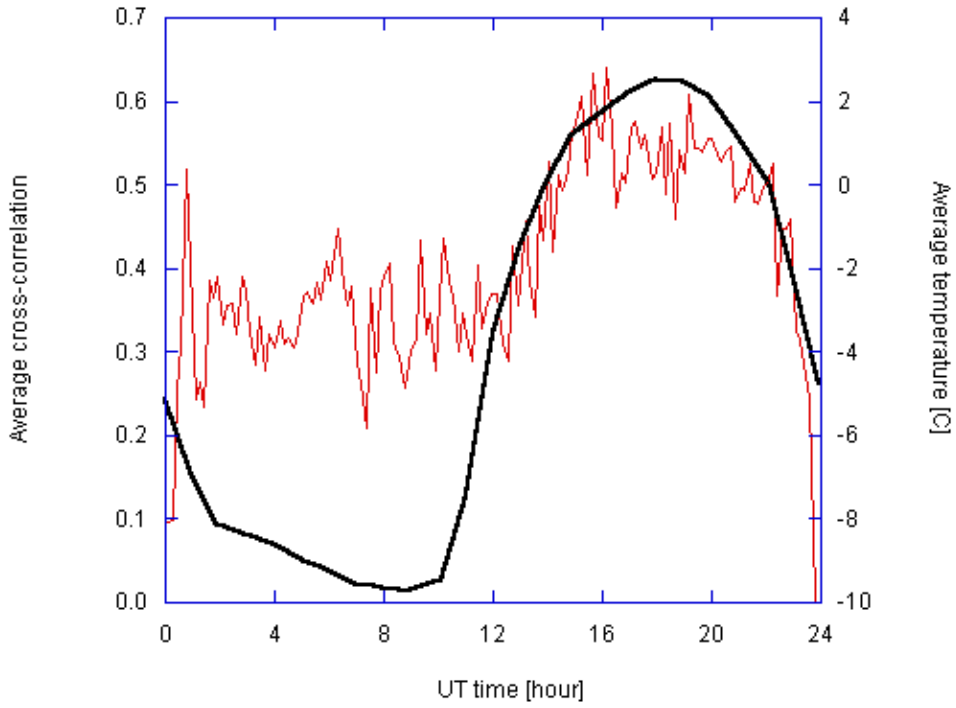

b)

Figure 9.- Average correlation coefficient for the period 1-21/11/99 compared with a) the average solar radiation (thick line), and b) the average temperature (thick line) for the same period.

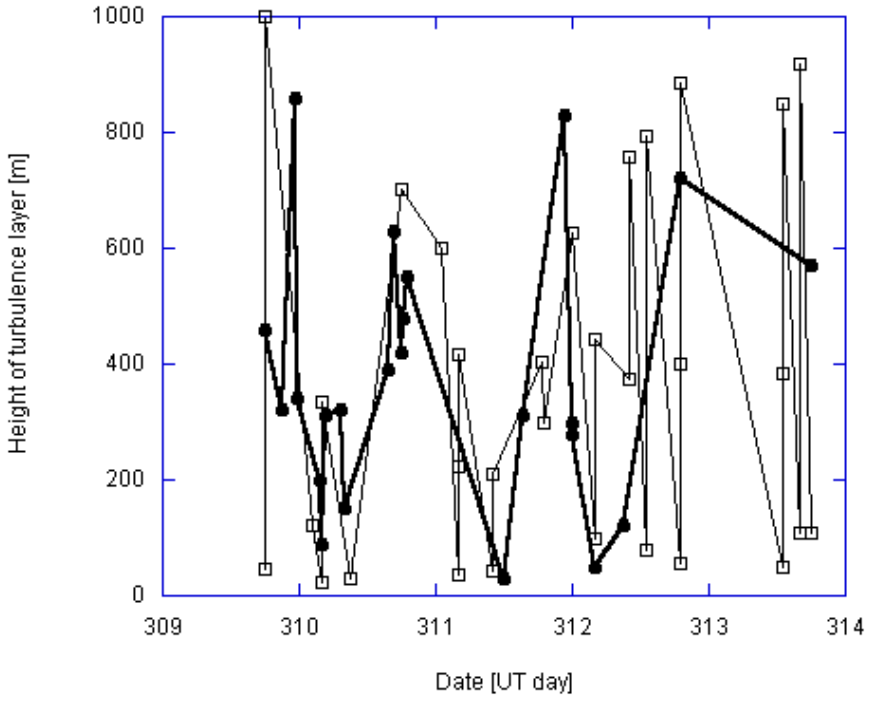

Figure 10.- Height of the turbulence layer calculated by direct radiosonde measurements (thin line) and the two-interferometer method (thick line). The dots indicate the measurements. UT day number 309 corresponds to November 5 1999.

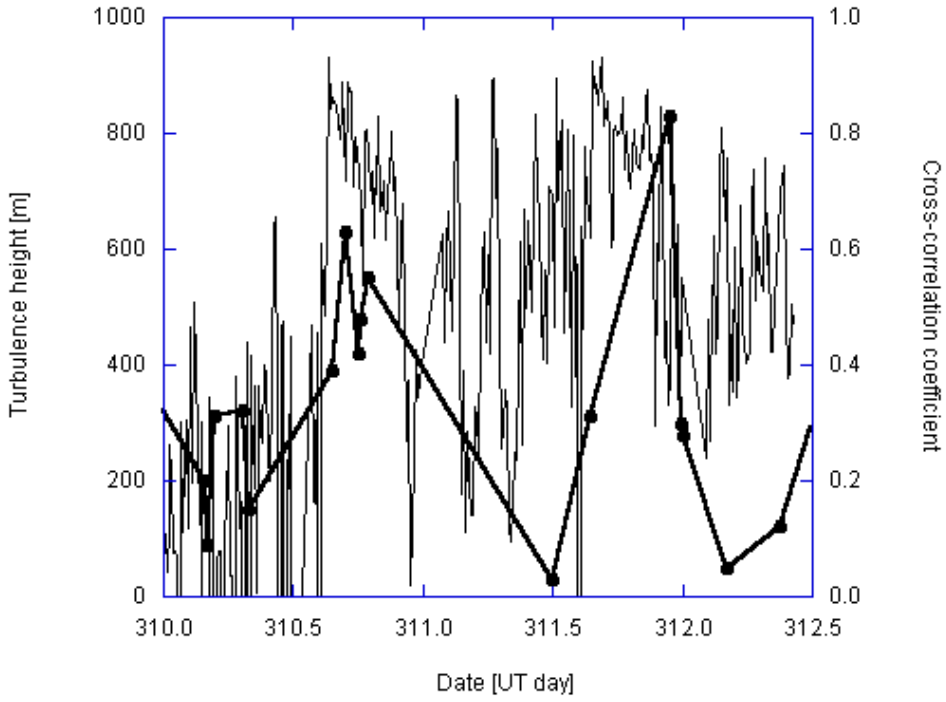

Figure 11.- Comparison between the cross-correlation coefficient between the interferometer and radiometer phase (thin line) and the height of the turbulence layer determined by the two-interferometer method (thick line). UT day number 310 corresponds to November 6 1999.